Two-dimensional atom localization via spontaneous emission in a coherently driven five-level M-type atomic system

Chunling Ding,[1,*] Jiahua Li,[1,†] Zhiming Zhan,[2] and Xiaoxue Yang[1]

[1]*Wuhan National Laboratory for Optoelectronics and School of Physics, Huazhong University of Science and Technology, Wuhan 430074, People's Republic of China*

[2]*School of Physics and Information Engineering, Jianghan University, Wuhan 430056, People's Republic of China*

(Received 23 March 2011; published 24 June 2011)

A scheme is proposed for two-dimensional atom localization in the subwavelength domain via controlled spontaneous emission. We consider a five-level M-type atomic system interacting with two orthogonal standing-wave laser fields and the vacuum of the radiation field. The interaction of the atom with space-dependent standing-wave fields can provide information about the position of the atom passing through, thus leading to atom localization. It is found that the localization is significantly improved due to the interference effect between the spontaneous decay channels and the dynamically induced quantum interference generated by the two standing-wave fields. By properly varying the system parameters, we can achieve high-precision and high-resolution atom localization.

DOI: 10.1103/PhysRevA.83.063834 PACS number(s): 42.50.Gy

I. INTRODUCTION

It is well known that measurement of the degree of atom localization has become an active research topic from both the theoretical and experimental points of view [1–5], because of its potential applications in various quantum optical effects such as laser cooling and trapping of neutral atoms [6,7], atom nanolithography [8,9], Bose-Einstein condensation [10,11], and so on. Some earlier works [12–15] regarding atom localization are based on the concept of virtual optical slits. In those schemes, the localization of an atom is determined by measuring the phase shift of the optical field in a cavity due to the spatially varying atom-field interaction. As is well known, atomic coherence and quantum interference can lead to some interesting phenomena, like giant Kerr nonlinearity [16,17], four-wave mixing (FWM) [18], electromagnetically induced transparency (EIT) [19], spontaneous emission enhancement or suppression [20–23], optical bistability (OB) [24,25], etc. For one-dimensional (1D) atom localization, many schemes [26–32] are also based on atomic coherence and quantum interference effects. For example, Herkommer and co-workers [28] proposed a scheme for 1D atom localization by using the measurement of the Autler-Townes spontaneous spectrum. Qamar *et al.* [29] put forward a simple scheme of 1D atom localization based on resonance fluorescence from a standing-wave field. Another related localization scheme was proposed by Paspalakis and co-workers [30,31] using measurement of the upper-state population for a three-level atom interacting with a classical standing-wave field and a weak probe laser field. Moreover, sub-half-wavelength localization [32] can be obtained via quantum interference in a four-level ladder-type atomic system. Alternatively, 1D atom localization can be realized via coherent manipulation of the Raman gain process [33]. Recently, Zubairy and colleagues discussed 1D atom localization using amplitude and phase control of the absorption spectrum [34,35].

Apart from the above-mentioned methods, other techniques [36–38] such as dark resonances or coherent population trapping (CPT) can also be used to achieve 1D atom localization. More recently, double-dark resonances have been used to realize two-dimensional (2D) atom localization [39]. Because there are more practical applications of this kind of 2D atom localization, many schemes have been put forward. For instance, Evers *et al.* [40] presented a 2D localization scheme for a quantum particle using multiple simultaneous dispersive interactions of the particle with two orthogonal standing-wave fields. A method for atom nanolithography based on 2D atom localization is reported in Ref. [41] by application of two orthogonal standing-wave fields. Ivanov and Rozhdestvensky [42] proposed a four-level tripod system for 2D atom localization by measuring the population of the atom in two standing-wave fields based on EIT. Afterward, Wan *et al.* proposed a scheme for 2D atom localization via quantum interference in a coherently driven inverted-Y atomic system [43] or via controlled spontaneous emission from a driven tripod system [44]. Inspired by these researches, we present a 2D atom localization scheme via controllable spontaneous emission in a coherently driven five-level M-type atomic system.

It has been reported that an M-type atomic system [45] with two closely spaced upper levels interacting with the same modes of the vacuum radiation field can exhibit an interference effect between the spontaneous decay channels, thus giving rise to greatly enhanced, suppressed, and quenched spontaneous emission line shapes. This leads us to pose another question: If a similar atomic system interacts with two orthogonal standing-wave fields rather than with two traveling-wave coupling fields, what will be the resulting atom localization when the atom passes through the standing-wave fields? Although 2D atom localization has been investigated in some schemes [39–44], most discussions are limited to considering the spontaneous emission in a single decay channel. In contrast, in this paper, we focus on the

*clding2006@126.com

†Author to whom correspondence should be addressed: huajia_li@163.com

measurement of spontaneous emission from two coherent decay channels, and thus we investigate 2D atom localization. With two spontaneous emission channels, there is potentially an improvement in the precision. Because of the spatial-position-dependent atom-field interaction, the spontaneously emitted photon carries information about the position probability distribution; as a result, the atom can be localized when the spontaneously emitted photon is detected. The detection of different frequencies of spontaneous emission allows us to determine different spatial structures of the filter function, such as wavelike, latticelike, mountainlike, and spikelike patterns. These interesting features result from the joint quantum interference effects, that is, the interference effect between the spontaneous decay channels owing to the two upper levels interacting with the same modes of the vacuum radiation field and the dynamically induced quantum interference which is created by two standing-wave laser fields. The field-induced quantum interference effects in two adjacent Λ-type structures are connected by vacuum-induced decay interference in our considered model. Consequently, we can achieve high-precision and high-resolution atom localization by adjusting the system parameters under the action of the dynamically induced decay-interference effects.

The remainder of this paper is organized as follows. In Sec. II, we present the atomic model under consideration and derive the conditional position probability distribution after interaction in the Raman-Nath regime. In Sec. III, we give a detailed analysis and explanation for the position distribution of the atom. Finally, our conclusions are summarized in Sec. IV.

II. THEORETICAL MODEL AND BASIC FORMULA

Let us consider a five-level M-type atomic configuration which consists of three lower levels $|0\rangle$, $|1\rangle$, and $|2\rangle$ and two upper levels $|3\rangle$ and $|4\rangle$ as depicted in Fig. 1. The atomic transitions from the upper levels $|3\rangle$ and $|4\rangle$ to the lower level $|0\rangle$ are coupled by vacuum modes (ω_λ) in free space. In addition, two orthogonal standing-wave laser fields are applied to drive the transitions $|3\rangle \leftrightarrow |1\rangle$ and $|4\rangle \leftrightarrow |2\rangle$, respectively. The corresponding Rabi frequencies are dependent on the

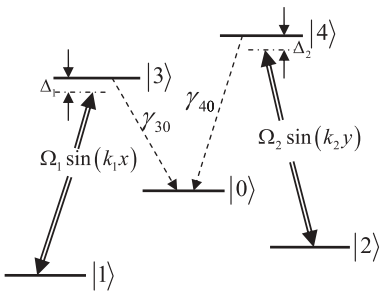

FIG. 1. Schematic diagram of a five-level M-type atomic system interacting with two orthogonal standing-wave fields. The five-level atomic model consists of two upper levels $|3\rangle$ and $|4\rangle$ and three lower levels $|0\rangle$, $|1\rangle$, and $|2\rangle$, in which two standing-wave fields are used to drive the transitions $|1\rangle \leftrightarrow |3\rangle$ and $|2\rangle \leftrightarrow |4\rangle$. Δ_1 and Δ_2 are respectively the detunings of the corresponding transitions. γ_{30} and γ_{40} are the decay rates from the two upper levels $|3\rangle$ and $|4\rangle$ to the lower level $|0\rangle$ in the free space.

position and can be defined by $\Omega_1 \sin(k_1 x)$ and $\Omega_2 \sin(k_2 y)$, with $k_1 = \omega_1/c$ and $k_2 = \omega_2/c$ being the wave vectors of the two fields. Therefore, the interaction between the atom and the standing-wave fields is space dependent on the x-y plane. Here we assume that the center-of-mass position of the atom along the directions of the standing-wave fields is nearly constant and neglect the kinetic part of the atom in the Hamiltonian by applying the Raman-Nath approximation [46]. Under these assumptions, the Hamiltonian which describes the dynamics of this system in the interaction picture and the rotating-wave approximation (RWA) can be written as (taking $\hbar = 1$)

$$\begin{aligned} H_I = {} & \Omega_1 \sin(k_1 x) e^{-i\Delta_1 t} |3\rangle\langle 1| + \Omega_2 \sin(k_2 y) e^{-i\Delta_2 t} |4\rangle\langle 2| \\ & + \sum_{\lambda e} g_{\lambda e}^{30} e^{-i\delta_{\lambda 3} t} |3\rangle\langle 0| \hat{b}_{\lambda e} \\ & + \sum_{\lambda e} g_{\lambda e}^{40} e^{-i\delta_{\lambda 4} t} |4\rangle\langle 0| \hat{b}_{\lambda e} + \text{H.c.}, \end{aligned} \tag{1}$$

where H.c. means the Hermitian conjugate. The quantities $\Delta_1 = \omega_1 - \omega_{31}$ and $\Delta_2 = \omega_2 - \omega_{42}$ stand for the frequency detunings of the coherent standing-wave field ω_i ($i = 1,2$) from the corresponding atomic resonance transition frequencies. $\delta_{\lambda j} = \omega_\lambda - \omega_{j0}$ ($j = 3,4$) represents the detuning between the λth vacuum mode and the resonance transition $|j\rangle \to |0\rangle$. Here λ and e denote the momentum vector and polarization of the emitted photons, respectively. $\hat{b}_{\lambda e}$ and $\hat{b}_{\lambda e}^\dagger$ are, respectively, the annihilation and creation operators for the λth vacuum mode with frequency ω_λ.

The dynamics of this system can be described by using the probability amplitude equations. Then the wave function of our considered system at time t can be expressed in terms of the state vectors as

$$\begin{aligned} |\Psi(t)\rangle = \int\int dx dy f(x,y)|x\rangle|y\rangle \big[& A_{1,0_\lambda}(x,y;t)|1,0_\lambda\rangle \\ & + A_{2,0_\lambda}(x,y;t)|2,0_\lambda\rangle + A_{3,0_\lambda}(x,y;t)|3,0_\lambda\rangle \\ & + A_{4,0_\lambda}(x,y;t)|4,0_\lambda\rangle + \sum_{\lambda e} A_{0,1_\lambda}(x,y;t)|0,1_\lambda\rangle \big], \end{aligned} \tag{2}$$

where the probability amplitude $A_{j,0_\lambda}(x,y;t)$ ($j = 1$–4) stands for the state of the atom at time t and $|0_\lambda\rangle$ implies that there is no emitted photon in the λth vacuum mode, $A_{0,1_\lambda}(x,y;t)$ gives the probability amplitude of finding the atom in level $|0\rangle$ with one emitted photon in the λth vacuum mode, and $f(x,y)$ is the center-of-mass wave function of the atom.

The 2D atom localization scheme in our system is based on the fact that the spontaneously emitted photon carries information about the position of the atom in the x-y plane due to the spatial-position-dependent interaction between the atom and standing-wave fields. Therefore, the measurement of the atomic position is conditioned on the detection of the frequency of the spontaneously emitted photon. When we have detected a spontaneously emitted photon at time t in the vacuum mode of wave vector λ, the atom is in its internal state $|0\rangle$ and the state vector of the system, after making appropriate projection over $\Psi(t)$, is simplified to

$$\begin{aligned} |\psi_{0,1_\lambda}\rangle &= \mathcal{N}\langle 0,1_\lambda|\Psi(t)\rangle \\ &= \mathcal{N}\int\int dx dy f(x,y)|x\rangle|y\rangle A_{0,1_\lambda}(x,y;t), \end{aligned} \tag{3}$$

where $\mathcal{N}$ is a normalization constant. Thus, the conditional position probability distribution, that is, the probability of finding the atom in the (x,y) position at time t, is

$$P(x,y;t|0,1_\lambda) = |\mathcal{N}|^2 \left|\langle x|\langle y|\psi_{0,1_\lambda}\rangle\right|^2 = |\mathcal{N}|^2 |f(x,y)|^2 \left|A_{0,1_\lambda}(x,y;t)\right|^2, \quad (4)$$

which can be derived from the probability amplitude $A_{0,1_\lambda}(x,y;t)$.

We now calculate an analytical expression for the probability amplitude $A_{0,1_\lambda}$ by solving the time-dependent Schrödinger wave equation $i\partial|\Psi(t)\rangle/\partial t = H_I|\Psi(t)\rangle$ with the interaction Hamiltonian [Eq. (1)] and the atomic wave function of our system [Eq. (2)]. The coupled equations of motion for the time evolution of the atomic probability amplitudes can be readily obtained as

$$i\frac{\partial A_{1,0_\lambda}(t)}{\partial t} = \Omega_1 \sin(k_1 x) e^{i\Delta_1 t} A_{3,0_\lambda}(t), \quad (5a)$$

$$i\frac{\partial A_{2,0_\lambda}(t)}{\partial t} = \Omega_2 \sin(k_2 y) e^{i\Delta_2 t} A_{4,0_\lambda}(t), \quad (5b)$$

$$i\frac{\partial A_{3,0_\lambda}(t)}{\partial t} = \Omega_1 \sin(k_1 x) e^{-i\Delta_1 t} A_{1,0_\lambda}(t) + \sum_{\lambda e} g_{\lambda e}^{30} e^{-i\delta_{\lambda 3} t} A_{0,1_\lambda}(t), \quad (5c)$$

$$i\frac{\partial A_{4,0_\lambda}(t)}{\partial t} = \Omega_2 \sin(k_2 y) e^{-i\Delta_2 t} A_{2,0_\lambda}(t) + \sum_{\lambda e} g_{\lambda e}^{40} e^{-i\delta_{\lambda 4} t} A_{0,1_\lambda}(t), \quad (5d)$$

$$i\frac{\partial A_{0,1_\lambda}(t)}{\partial t} = g_{\lambda e}^{03} e^{i\delta_{\lambda 3} t} A_{3,0_\lambda}(t) + g_{\lambda e}^{04} e^{i\delta_{\lambda 4} t} A_{4,0_\lambda}(t). \quad (5e)$$

We proceed by performing a formal time integration of Eq. (5e) with respect to t' and substitute the results into Eqs. (5c) and (5d) to eliminate $A_{0,1_\lambda}(t)$; then we obtain the integro-differential equations

$$\frac{\partial A_{3,0_\lambda}(t)}{\partial t} = -i\Omega_1 \sin(k_1 x) e^{-i\Delta_1 t} A_{1,0_\lambda}(t) - \int_0^t K_{33}(t-t') A_{3,0_\lambda}(t') dt' - \int_0^t e^{-i\omega_{43} t} K_{34}(t-t') A_{4,0_\lambda}(t') dt', \quad (6a)$$

$$\frac{\partial A_{4,0_\lambda}(t)}{\partial t} = -i\Omega_2 \sin(k_2 y) e^{-i\Delta_2 t} A_{2,0_\lambda}(t) - \int_0^t e^{i\omega_{43} t} K_{43}(t-t') A_{3,0_\lambda}(t') dt' - \int_0^t K_{44}(t-t') A_{4,0_\lambda}(t') dt', \quad (6b)$$

where $K_{jl}(t-t')$ $(j,l = 3,4)$ is the delay Green function with definition

$$K_{jl}(t-t') = \sum_{\lambda e} g_{\lambda e}^{j0} g_{\lambda e}^{0l} e^{-i\delta_{\lambda l}(t-t')}. \quad (7)$$

Since the atomic transitions from the two upper levels to the lower level $|0\rangle$ are coupled by the reservoir of free vacuum modes, the process is Markovian, so we can apply the Weisskopf-Wigner theory [47] to obtain

$$K_{jl}(t-t') = \frac{p_{jl}}{2}\sqrt{\gamma_{j0}\gamma_{l0}}\,\delta(t-t'), \quad (8)$$

with $p_{jl} = \delta_{jl} + p(1-\delta_{jl})$; here δ_{jl} is the Krönecker delta function, p $(0 \leqslant p \leqslant 1)$ represents the quantum interference in the atomic transitions coupled to the free vacuum modes and is given by $p = \frac{\vec{\mu}_{30}\cdot\vec{\mu}_{40}}{|\vec{\mu}_{30}||\vec{\mu}_{40}|}$, and $\vec{\mu}_{30}$ and $\vec{\mu}_{40}$ stand for the dipole-matrix moments correspond to the transitions $|3\rangle \to |0\rangle$ and $|4\rangle \to |0\rangle$, respectively. Obviously, the existence of quantum interference depends on the nonorthogonality of dipole matrix elements $\vec{\mu}_{30}$ and $\vec{\mu}_{40}$. When the two dipole-matrix moments are orthogonal, $p = 0$, implying that there is no quantum interference between the two transitions; when the dipole-matrix moments are parallel or antiparallel, $p = 1$, indicating that the quantum interference is maximal between the two transitions; otherwise, $0 < p < 1$. γ_{j0} and γ_{l0} denote the decay rates from the levels $|j\rangle$ and $|l\rangle$ to the lower level $|0\rangle$ in the free space, respectively.

By applying the Laplace transform method and the final value theorem, the probability amplitude $A_{0,1_\lambda}$ in the long time limit can be obtained as

$$A_{0,1_\lambda}(x,y;t\to\infty) = -ig_{\lambda e}^{03}\tilde{A}_{3,0_\lambda}(s=-i\delta_{\lambda 3}) - ig_{\lambda e}^{04}\tilde{A}_{4,0_\lambda}(s=-i\delta_{\lambda 4}), \quad (9)$$

where $\tilde{A}_{j,0_\lambda}(s)$ $(j = 3,4)$ is the Laplace transform of $A_{j,0_\lambda}(t)$ with $s = -i\delta_{\lambda j}$.

Next, by carrying out the Laplace transformations for Eqs. (5a), (5b), (6a), and (6b), we have the results

$$\tilde{A}_{3,0_\lambda}(s=-i\delta_{\lambda 3}) = \frac{BC - p\frac{\sqrt{\gamma_{30}\gamma_{40}}}{2}D}{AB - p^2\frac{\gamma_{30}\gamma_{40}}{4}}, \quad (10a)$$

$$\tilde{A}_{4,0_\lambda}(s=-i\delta_{\lambda 4}) = \frac{AD - p\frac{\sqrt{\gamma_{30}\gamma_{40}}}{2}C}{AB - p^2\frac{\gamma_{30}\gamma_{40}}{4}}, \quad (10b)$$

where

$$A = \frac{\gamma_{30}}{2} - i\delta_{\lambda 3} + \frac{i\Omega_1^2\sin^2(k_1 x)}{\delta_{\lambda 3} - \Delta_1},$$

$$B = \frac{\gamma_{40}}{2} - i\delta_{\lambda 4} + \frac{i\Omega_2^2\sin^2(k_2 y)}{\delta_{\lambda 4} - \Delta_2},$$

$$C = A_{3,0_\lambda}(0) + \frac{\Omega_1\sin(k_1 x)}{\delta_{\lambda 3} - \Delta_1}A_{1,0_\lambda}(0),$$

$$D = A_{4,0_\lambda}(0) + \frac{\Omega_2\sin(k_2 y)}{\delta_{\lambda 4} - \Delta_2}A_{2,0_\lambda}(0).$$

Finally, the conditional probability of finding the atom in level $|0\rangle$ with a spontaneously emitted photon of frequency ω_λ in the vacuum mode λ is then given by

$$P(x,y;t\to\infty|0,1_\lambda) = |\mathcal{N}|^2|f(x,y)|^2\left|A_{0,1_\lambda}(x,y;t\to\infty)\right|^2 = |\mathcal{N}|^2|f(x,y)|^2\left|g_{\lambda e}^{03}\tilde{A}_{3,0_\lambda}(s=-i\delta_{\lambda 3}) + g_{\lambda e}^{04}\tilde{A}_{4,0_\lambda}(s=-i\delta_{\lambda 4})\right|^2. \quad (11)$$

Due to the center-of-mass wave function of the atom $f(x,y)$ is assumed to be nearly constant over many wavelengths of the standing-wave fields in the x-y plane, the conditional position probability distribution $P(x,y;t\to\infty|0,1_\lambda)$ is determined by

the last term in Eq. (11). From this, we can define the filter function as

$$\begin{aligned} F(x,y) &= \left|g_{\lambda e}^{03}\tilde{A}_{3,0_\lambda}(s=-i\delta_{\lambda 3})+g_{\lambda e}^{04}\tilde{A}_{4,0_\lambda}(s=-i\delta_{\lambda 4})\right|^2 \\ &= \gamma_{30}\left|\tilde{A}_{3,0_\lambda}(s=-i\delta_{\lambda 3})\right|^2+\gamma_{40}\left|\tilde{A}_{4,0_\lambda}(s=-i\delta_{\lambda 4})\right|^2 \\ &\quad + p\sqrt{\gamma_{30}\gamma_{40}}\left[\tilde{A}_{3,0_\lambda}(s=-i\delta_{\lambda 3})\tilde{A}^*_{4,0_\lambda}(s=-i\delta_{\lambda 4})\right. \\ &\quad \left.+\tilde{A}^*_{3,0_\lambda}(s=-i\delta_{\lambda 3})\tilde{A}_{4,0_\lambda}(s=-i\delta_{\lambda 4})\right]. \end{aligned} \tag{12}$$

Equation (12) shows that the conditional position probability distribution depends on the detunings of the standing-wave driving fields and the population in the upper or lower levels, as well as the frequency of spontaneously emitted photon. As a consequence, we can obtain the position information of the atom by measuring the spontaneous emission under proper conditions.

III. RESULTS AND DISCUSSION

In this section, we analyze the conditional position probability distribution of the atom via a few numerical calculations based on the filter function $F(x,y)$ from Eq. (12), and then demonstrate 2D atom localization by detecting the frequency of spontaneously emitted photons in mode λ. It is evident that the filter function $F(x,y)$ depends not only on the frequency of the spontaneously emitted photon and the parameters of the two standing-wave driving fields, but also on the initial atomic state and the quantum interference effects. There exist two possible types of quantum interference in our system, that is, (I) the quantum interference effect between the spontaneous decay channels due to the two upper levels interacting with the same vacuum modes and (II) the dynamically induced quantum interference generated by the two standing-wave fields. Therefore, a variety of atom localization features can be controlled by the two standing-wave fields, the joint quantum interferences, and the preparation of the initial quantum state of the atom. All the parameters used in this paper are in units of the decay rate γ_{30}. In the following discussion, we use some of the detuning parameters, in which δ_λ is the detuning of the radiation field from the middle of the two upper levels, i.e., $\delta_\lambda = \omega_\lambda - 0.5(\omega_{30}+\omega_{40}) = \delta_{\lambda 3} - 0.5\omega_{43} = \delta_{\lambda 4} + 0.5\omega_{43}$; here $\omega_{43} = \omega_{40} - \omega_{30}$ is the frequency difference of the two upper levels.

First, we consider the case where the atom is initially prepared in level $|3\rangle$, i.e., $A_{3,0_\lambda}(0) = 1$, and there is no quantum interference between the two spontaneous decay channels (i.e., $p = 0$). For the sake of simplicity, we first limit our discussion to the resonant coupling situation, that is, both the orthogonal standing-wave fields are on resonance with respect to the corresponding transitions. Under these conditions, the maxima of the filter function are located at $k_1 x = \pm\arcsin(\frac{\delta_\lambda+0.5\omega_{43}}{\Omega_1}) + n\pi$, where n is an integer. In Fig. 2, we show a three-dimensional plot of the filter function $F(x,y)$ as a function of the normalized positions $(k_1 x, k_2 y)$. It can be clearly seen that the peaks of atom localization along the y axis have a wavelike pattern. The very narrow wavelike peaks are achieved when the detuning δ_λ is small [see Figs. 2(a) and 2(b)], especially in the resonance condition [i.e., $\delta_\lambda = 0$ in Fig. 2(a)] $k_1 x \simeq 0, \pm\pi$. In a period of $[-\pi, +\pi]$, which corresponds to three localization peaks as shown in Fig. 2(a),

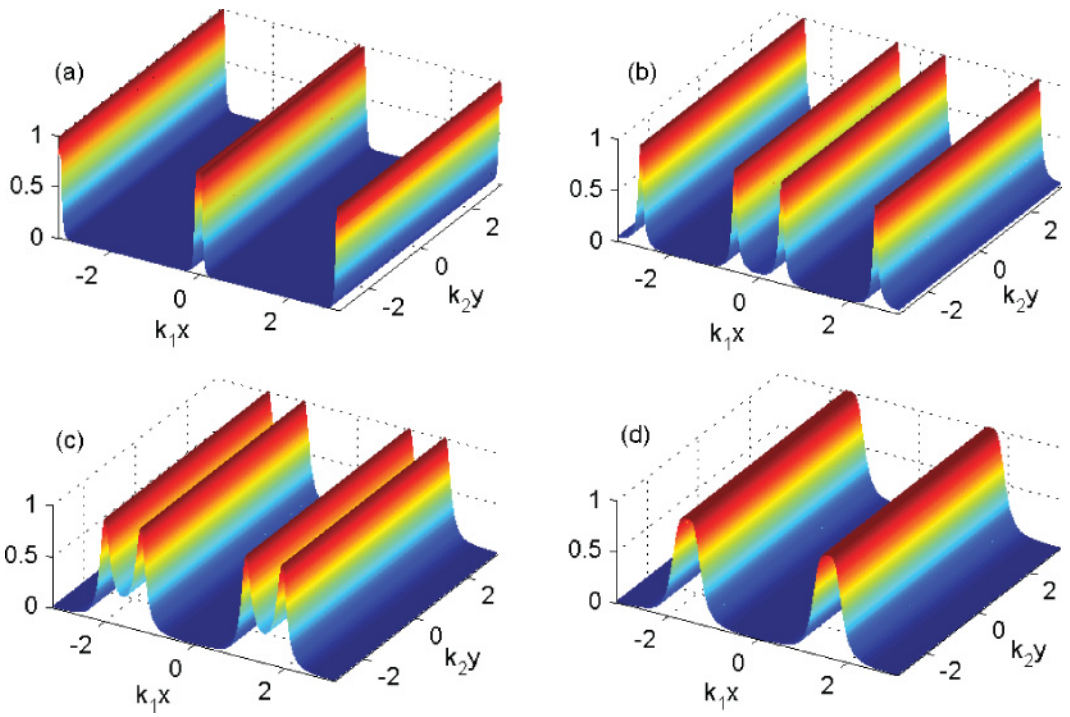

FIG. 2. (Color online) The filter function $F(x,y)$, which directly reflects the conditional position probability distribution, as a function of $(k_1 x, k_2 y)$ in dependence on the detuning of the spontaneously emitted photon. (a) $\delta_\lambda = 0$; (b) $\delta_\lambda = 4.25$; (c) $\delta_\lambda = 8.25$; (d) $\delta_\lambda = 9$. The other parameters used are $\Omega_1 = 9.5$, $\Omega_2 = 10.5$, $\Delta_1 = \Delta_2 = 0$, $\gamma_{30} = \gamma_{40} = 2$, $\omega_{43} = 1.0$, and $p = 0$. The atom is initially prepared in level $|3\rangle$, i.e., $A_{3,0_\lambda}(0) = 1$. All parameters in this paper are in units of γ_{30}.

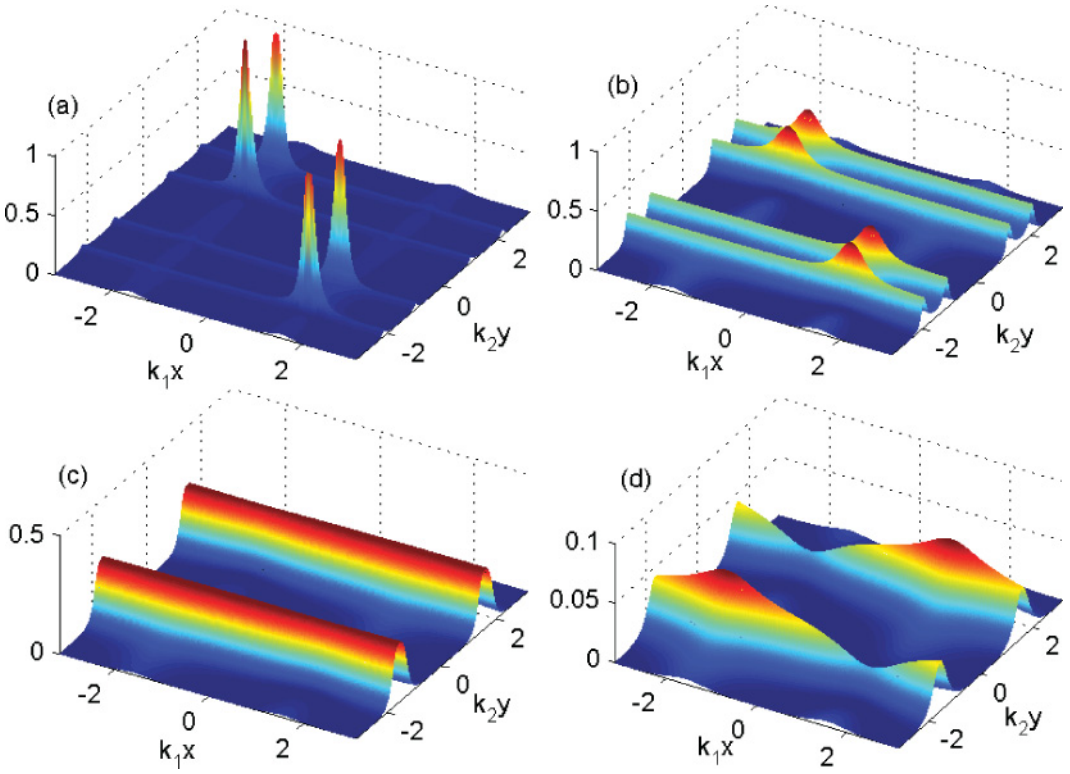

FIG. 3. (Color online) The filter function $F(x,y)$ as a function of (k_1x,k_2y) in dependence on the detuning of the spontaneously emitted photon. (a) $\delta_\lambda = 9.2$; (b) $\delta_\lambda = 10$; (c) $\delta_\lambda = 11$; (d) $\delta_\lambda = 12$. The system parameters used are the same as in Fig. 2 except that $p = 1$ and the atom is initially prepared in a superposition state of $|1\rangle$ and $|2\rangle$, i.e., $A_{1,0_\lambda}(0) = A_{2,0_\lambda}(0) = 1/\sqrt{2}$.

the atom is localized around the nodes of the standing-wave field $\Omega_1 \sin(k_1x)$, and thus we obtain high precision and high resolution in the conditional position probability distribution of the atom. When the detuning parameter is tuned to $\delta_\lambda = 4.25$, the atom is localized at the positions $k_1x = \pm\pi/6, \pm 5\pi/6$ as shown in Fig. 2(b). As can be seen from Figs. 2(a) and 2(b), we can achieve much better localization precision than for the wavelike pattern reported in Refs. [39,42]. As a matter of fact, this kind of high-precision and high-resolution 2D atom localization can be attributed to the dynamically induced interference effect between the two pathways $|+\rangle_3 \to |0\rangle$ and $|-\rangle_3 \to |0\rangle$, in which the levels $|\pm\rangle_3$ are the dressed-state sublevels generated by the resonant driving field $\Omega_1 \sin(k_1x)$. When there is an increase in the detuning δ_λ [e.g., $\delta_\lambda = 8.25$ in Fig. 2(c)], we have $1/2 < \sin^2(k_1x) < 1$; therefore, the two peaks located at the same side of the coordinates are close to each other as shown in Fig. 2(c). Furthermore, when the detuning is detected at an appropriate value, i.e., $\delta_\lambda = 9$, we obtain $\sin(k_1x) = \pm 1$; four maxima merge into two and lie on the antinodes of the standing-wave field which is aligned along the y axis [see Fig. 2(d)]. At the same time, the width of the wavelike peaks becomes larger, which indicates that the resolution of atom localization is reduced.

These results imply that there is a strong correlation between the frequency of the spontaneously emitted photon and the position of the atom. The measurement of a particular frequency corresponds to the localization of the atom within a subwavelength region of the standing-wave field. Moreover, when the atom is prepared in the upper state $|3\rangle$, because there is no quantum interference between the two decay channels (i.e., $p = 0$), the population in level $|3\rangle$ cannot be transferred into level $|4\rangle$ in the absence of the decay-interference effect. Therefore, only the decay from level $|3\rangle$ affects the atom localization. When the emitted photon is detected at nonresonance with the middle of the two upper levels, the destructive quantum interference between the two pathways $|+\rangle_3 \to |0\rangle$ and $|-\rangle_3 \to |0\rangle$ leads to a spectral valley at $k_1x = n\pi$ with n being an arbitrary integer.

In the following, let us consider the case that the atom is initially prepared in a coherent superposition state of two ground levels $\Psi(0) = (|1\rangle + |2\rangle)/\sqrt{2}$, that is, $A_{1,0_\lambda}(0) = A_{2,0_\lambda}(0) = 1/\sqrt{2}$. Moreover, there exists quantum interference between the spontaneous decay channels coupled to the free vacuum reservoir (i.e., $p = 1$). Figure 3 displays the filter function $F(x,y)$ versus the normalized positions (k_1x,k_2y) in such a case. As can be seen, the localization of the atom is different from the situation discussed above because of the combined action of the standing-wave fields and the vacuum-induced decay-interference effect. The specific results are as follows. The conditional position probability is distributed mostly in the second and fourth quadrants [$\sin(k_1x)\sin(k_2y) < 0$] of the x-y plane with a sharp double-peak structure as shown in Fig. 3(a), that is, the atom is localized at $k_1x = (2m+1)\pi/2$ and $k_2y = (2n+1)\pi/4$ (m,n are integers) in the second and fourth quadrants. These phenomena are opposite to those reported in Ref. [44]. In Fig. 3(a) the sharp double-peak structure is caused by the decay-interference effects in the pathways $|+\rangle_3 \to |0\rangle \to |+\rangle_4$ and $|-\rangle_3 \to |0\rangle \to |+\rangle_4$; the other double-peak structure results from the quantum

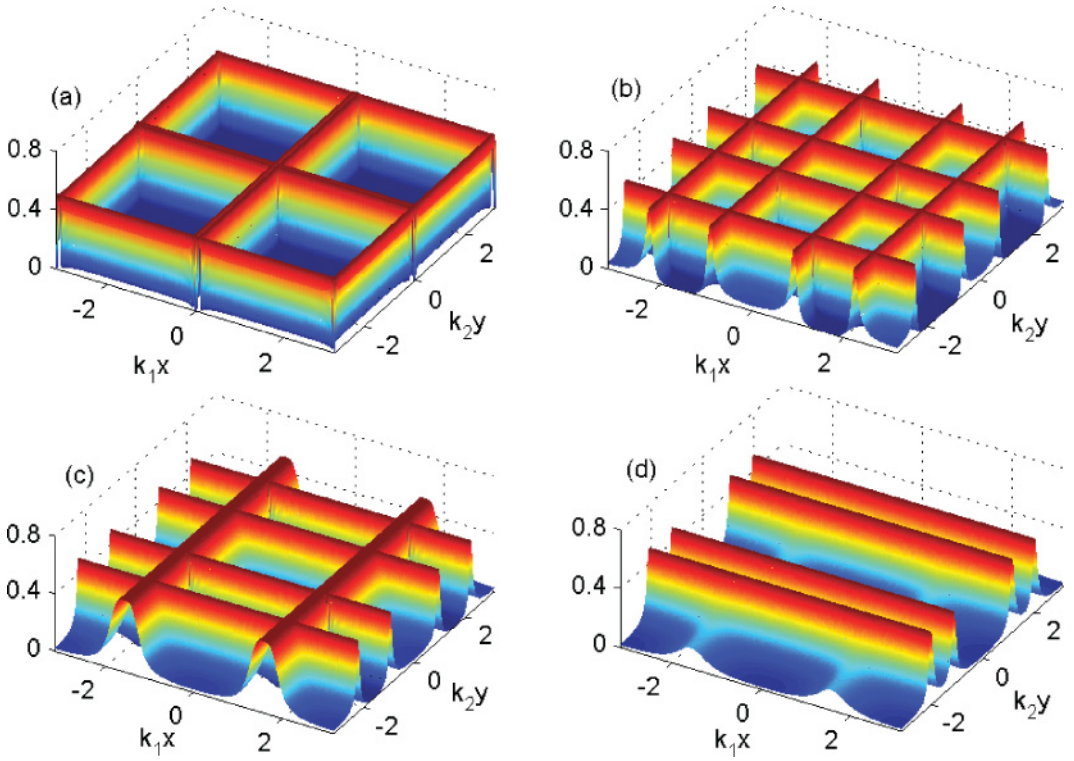

FIG. 4. (Color online) The filter function $F(x,y)$ as a function of (k_1x,k_2y) in dependence on the detuning of the spontaneously emitted photon. (a) $\delta_\lambda = 0$; (b) $\delta_\lambda = 7$; (c) $\delta_\lambda = 9$; (d) $\delta_\lambda = 10$. The system parameters used are the same as in Fig. 3 except that the atom is initially prepared in a superposition state of $|3\rangle$ and $|4\rangle$, i.e., $A_{3,0_\lambda}(0) = A_{4,0_\lambda}(0) = 1/\sqrt{2}$.

interference between the pathways $|+\rangle_3 \rightarrow |0\rangle \rightarrow |-\rangle_4$ and $|-\rangle_3 \rightarrow |0\rangle \rightarrow |-\rangle_4$. Here, $|\pm\rangle_4$ are the dressed-state sublevels generated by the resonant driving fields $\Omega_2 \sin(k_2 y)$. Hence we obtain a higher probability of finding the atom in the second and fourth quadrants for a frequency measurement of the spontaneous emission when the emitted photon has a relatively small detuning. As the detuning δ_λ increases, the spontaneous emission is gradually suppressed, which results in a decrease in the value of the filter function $F(x,y)$ [see Figs. 3(b)– 3(d)]. It is shown that the peaks of atom localization in this condition occur at the antinodes of the standing-wave field propagating along the x axis [see Fig. 3(c)], which is completely opposite to the situation when the atom is initially prepared in level $|3\rangle$ (see Fig. 2). Therefore, the wavelike localization peaks are aligned along the x axis. In addition, the high-precision localization is destroyed when the frequency of the spontaneously emitted photon is large enough [see Fig. 3(d)]. As a result, when the atom is trapped in the two ground levels (i.e., $|1\rangle$ and $|2\rangle$), the precision of the atom localization is dependent on the frequency of the spontaneously emitted photon. High-precision and high-resolution 2D atom localization can be obtained only when the emitted photon is near resonance with the corresponding atomic transition. This is due to the fact that the vacuum-induced quantum interference between the two spontaneous decay channels decreases with an increase in the detuning of the radiation field from the middle of the two upper levels.

In order to explore the effect of the initial population of the two upper levels on the atom localization, we plot in Fig. 4 the filter function $F(x,y)$ versus the normalized positions (k_1x,k_2y) for different detuning values when the atom is initially prepared in a coherent superposition state of the two upper levels, i.e., $\Psi(0) = (|3\rangle + |4\rangle)/\sqrt{2}$. When a spontaneously emitted photon with frequency $\omega_\lambda = (\omega_{30} + \omega_{40})/2$ is detected, the filter function in Fig. 4(a) displays a normalized latticelike pattern, and the atom is localized at the edges of these lattices. Because the atom is localized at the nodes of the two standing-wave fields, such a latticelike pattern is better than that proposed in Refs. [39,43,44]. When the detuning is increased to $\delta_\lambda = 7$, the maxima of the filter function can be found in the region between the node and antinode of the standing-wave field [see Fig. 4(b)]. With a further increase of the detuning δ_λ, the two localization peaks move toward the antinodes of the standing-wave field along the x axis, and the four peaks merge into two and are located at the antinodes of the standing-wave field as shown in Fig. 4(c), whereas the atom localized at $k_2 y = (2n+1)\pi/6$ (n is an integer) is slightly shifted toward the antinode. Finally, when $\delta_\lambda = 10$, the localization peaks along the y axis are greatly suppressed; at the same time, the peaks of localization along the x axis are close to the antinodes of the standing-wave field [see Fig. 4(d)]. Distribution of the localization peaks takes a form similar to that shown in Fig. 3(b); the difference is that the degree of atom localization is larger than in the situation in Fig. 3(b). Because the heights of the wavelike peaks for all values of the position are the same, and thus we obtain a uniform position distribution. Because the atom is prepared in an equal superposition of the upper levels $|3\rangle$ and $|4\rangle$, the spontaneous emission remains unchanged all the while, and the

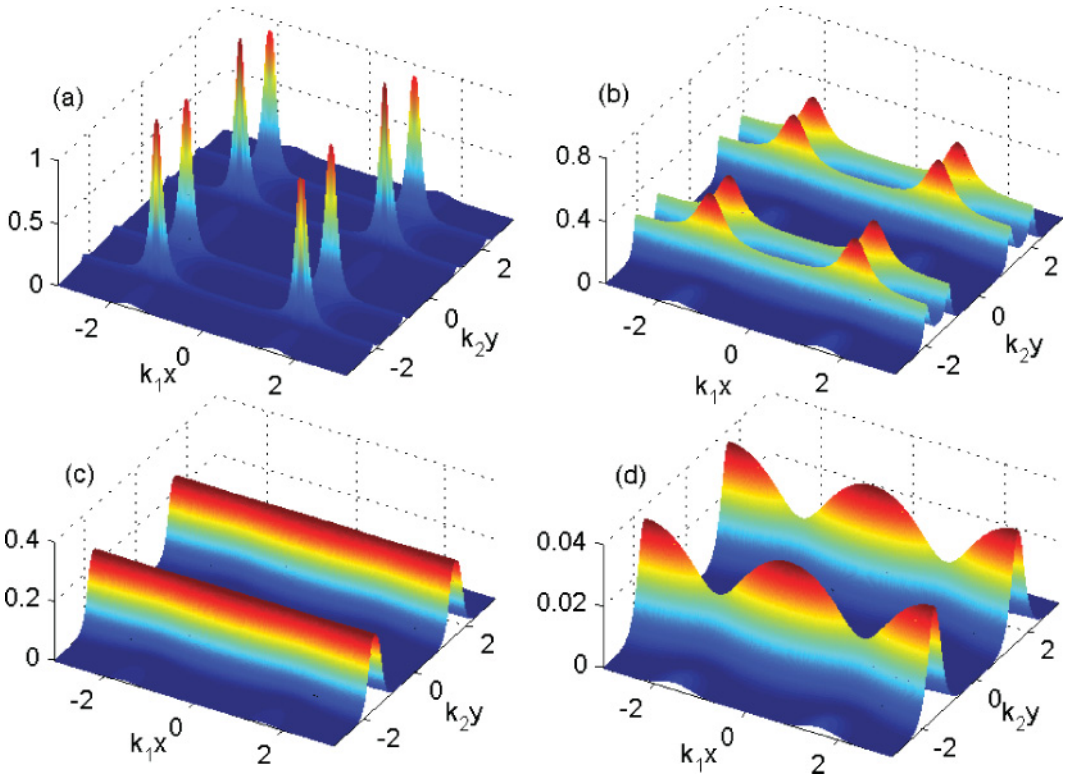

FIG. 5. (Color online) The filter function $F(x,y)$ as a function of (k_1x,k_2y) in dependence on the detuning of the spontaneously emitted photon. (a) $\delta_\lambda = 9.2$; (b) $\delta_\lambda = 10$; (c) $\delta_\lambda = 11$; (d) $\delta_\lambda = 12$. The system parameters used are the same as in Fig. 3 except that the atom is initially prepared in a superposition state of $|3\rangle$ and $|4\rangle$, i.e., $A_{3,0_\lambda}(0) = 1/\sqrt{2}$ and $A_{4,0_\lambda}(0) = -1/\sqrt{2}$.

joint quantum interference induced by the vacuum radiation field and the two standing-wave fields affects the position of atom localization.

In order to further explicitly show the influences of the initial atomic state on the 2D atom localization, we consider the case that the atom is initially prepared in another coherent superposition state of the two upper levels, that is, $\Psi(0) = (|3\rangle - |4\rangle)/\sqrt{2}$. In Fig. 5, we present the results for the conditional position probability distribution of the atom. When detecting the detuning $\delta_\lambda = 9.2$, the filter function $F(x,y)$ reaches maxima at positions around $k_1x = (2m+1)\pi/2$ and $k_2y = (2n+1)\pi/4$ (m, n are integers) as shown in Fig. 5(a). In this case, the atom is localized at these sharp peaks. As can be seen from Figs. 3(a) and 5(a), this kind of high-precision and high-resolution atom localization cannot be observed in those schemes which employ only single-channel spontaneous emission [40–44]. When the frequency detuning is slightly increased, i.e., $\delta_\lambda = 10$, these enhanced localization peaks are strongly suppressed, as shown in Fig. 5(b). As in the earlier discussions, with an increase in detuning δ_λ, four wavelike peaks of atom localization along the x axis evolve into two and are situated at the antinodes of the standing-wave field [see Fig. 5(c)]. As can be seen from Fig. 5(d), the filter function $F(x,y)$ has a mountainlike pattern when the spontaneously emitted photon is at a particular frequency. Moreover, the maxima of the localization peaks are greatly inhibited. As a result, the atom localization will completely disappear when a large frequency detuning from the emitted photon and the middle of the two upper levels is detected. Therefore, in order to obtain high-precision and high-resolution 2D atom localization, the spontaneously emitted photon should be at resonance with the middle of the two upper levels as much as possible.

Here we mention again that the above discussions about 2D atom localization refer to on-resonance conditions, i.e., the two standing-wave fields are resonant with the corresponding atomic transitions. Under nonresonant conditions, the behavior of atom localization differs considerably from the results observed above and is of special interest. Now we investigate the effects of the detunings of two standing-wave fields on the 2D atom localization. By choosing proper parameters, as can be seen from Fig. 6, we can achieve high-precision and high-resolution atom localization. Figure 6(a) displays the resulting filter function $F(x,y)$ in the case of $\Delta_1 = \Delta_2 = 3.5$, which describes a latticelike pattern with the atom localized at the edges of these lattices. More interestingly, when the detunings of the two standing-wave fields are tuned to $\Delta_1 = \Delta_2 = 4.5$, the peaks of atom localization along the x axis completely vanish, while the localization peaks along the y axis become quite sharp, as shown in Fig. 6(b), and lie near the nodes of the standing-wave field. In contrast, when $\Delta_1 = \Delta_2 = 5.5$, the peaks of atom localization lie along the x axis and are located around the nodes of the standing-wave field $\Omega_2 \sin(k_2y)$ [see Fig. 6(c)]. Moreover, these localization peaks are greatly suppressed and become wider. It can be seen from Fig. 6(d) that when the detunings of the two standing-wave fields are adjusted to $\Delta_1 = \Delta_2 = 6.5$, the filter function $F(x,y)$ exhibits a spikelike pattern and has maxima at positions corresponding to the intersections of nodes. Consequently, high-precision localization is achieved for small values of the detunings.

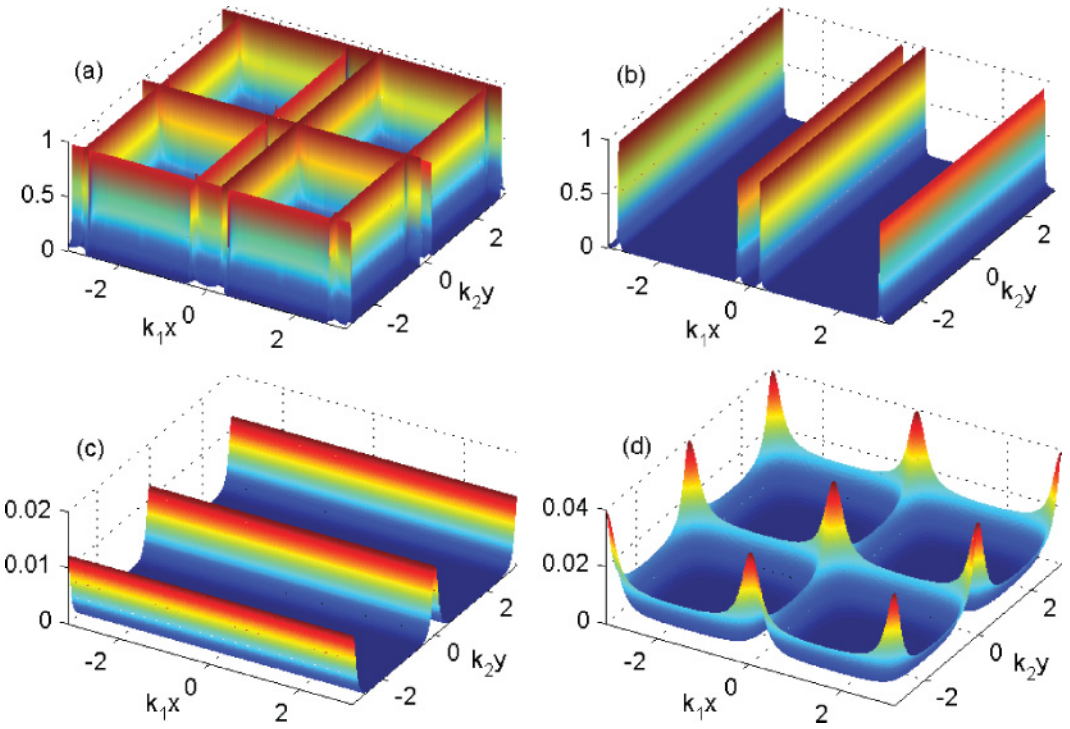

FIG. 6. (Color online) The filter function $F(x,y)$ as a function of (k_1x,k_2y) for different detunings of the two standing-wave laser fields. (a) $\Delta_1 = \Delta_2 = 3.5$; (b) $\Delta_1 = \Delta_2 = 4.5$; (c) $\Delta_1 = \Delta_2 = 5.5$; (d) $\Delta_1 = \Delta_2 = 6.5$. The system parameters used are the same as in Fig. 5 except that $\gamma_{30} = \gamma_{40} = 1$ and $\delta_\lambda = 5$.

From the above discussions of Figs. 5 and 6, we can see that the filter function $F(x,y)$ has a small value when a large detuning between the emitted photon and the atomic transition is detected or when the two standing-wave fields are placed far of resonance. This is mainly due to the suppression of the spontaneous emission, which is caused by both the decay-interference effect and the field-induced interference effect.

IV. CONCLUSIONS

In conclusion, we have investigated the conditional position probability distribution of a five-level M-type atom as it passes through two orthogonal standing-wave laser fields, based on the phenomena of spontaneous emission. Owing to the spatial-position-dependent atom-field interaction, 2D atom localization can be achieved by the detection of the spontaneously emitted photon. Therefore, the measurement of the spontaneous emission gives immediate information about the position of the atom and determines the different spatial structures of the filter function, such as wavelike, latticelike, mountainlike, and spikelike patterns. These phenomena originate from the quantum interference effects induced by the vacuum radiation field and the two standing-wave fields. We have shown that the precision of atom localization depends upon the initial-state preparation and the detunings of the two standing-wave fields. The proper preparation of the initial state and choice of the frequencies of the two standing-wave fields leads to spectral line narrowing of the spontaneous emission. The resolution of the localization peaks can be increased by changing the relevant frequency of the standing-wave fields. As a consequence, the atom can be localized with a high precision and resolution within a certain range. It should be pointed out that, although the spontaneous emission is a random process in nature and would require the use of 4π detectors in principle, it is not necessary to measure every atom for practical purposes.

ACKNOWLEDGMENTS

We would like to thank Professor Ying Wu for helpful discussion and his encouragement. The research is in part supported by the National Natural Science Foundation of China (Grants No. 10975054, No. 91021011, and No. 11004069), by the Doctoral Foundation of the Ministry of Education of China under Grants No. 200804870051 and No. 20100142120081, by the Innovation Foundation from Huazhong University of Science and Technology under Grant No. 2010MS074, and by Scientific Research Program of Hubei Provincial Department of Education under Grant No. Q20104501.

[1] R. Quadt, M. Collett, and D. F. Walls, Phys. Rev. Lett. **74**, 351 (1995).
[2] A. M. Herkommery, H. J. Carmichaelz, and W. P. Schleich, Quantum Semiclass. Opt. **8**, 189 (1996).
[3] G. Rempe, Appl. Phys. B **60**, 233 (1995).
[4] S. Kunze, K. Dieckmann, and G. Rempe, Phys. Rev. Lett. **78**, 2038 (1997).
[5] P. Rudy, R. Ejnisman, and N. P. Bigelow, Phys. Rev. Lett. **78**, 4906 (1997).
[6] H. Metcalf and P. Van der Straten, Phys. Rep. **244**, 203 (1994).

[7] W. D. Phillips, Rev. Mod. Phys. **70**, 721 (1998).
[8] K. S. Johnson, J. H. Thywissen, W. H. Dekker, K. K. Berggren, A. P. Chu, R. Younkin, and M. Prentiss, Science **280**, 1583 (1998).
[9] A. N. Boto, P. Kok, D. S. Abrams, S. L. Braunstein, C. P. Williams, and J. P. Dowling, Phys. Rev. Lett. **85**, 2733 (2000).
[10] G. P. Collins, Phys. Today **49**, 18 (1996).
[11] Y. Wu and R. Côté, Phys. Rev. A **65**, 053603 (2002).
[12] P. Storey, M. Collett, and D. Walls, Phys. Rev. Lett. **68**, 472 (1992).
[13] P. Storey, M. Collett, and D. Walls, Phys. Rev. A **47**, 405 (1993).
[14] P. Storey, T. Sleator, M. Collett, and D. Walls, Phys. Rev. A **49**, 2322 (1994).
[15] S. Kunze, G. Rempe, and M. Wilkens, Europhys. Lett. **27**, 115 (1994).
[16] H. Wang, D. Goorskey, and M. Xiao, Phys. Rev. Lett. **87**, 073601 (2001).
[17] Y. Wu and X. Yang, Appl. Phys. Lett. **91**, 094104 (2007).
[18] Y. Wu and X. Yang, Phys. Rev. A **70**, 053818 (2004).
[19] Y. Wu, L. L. Wen, and Y. F. Zhu, Opt. Lett. **28**, 631 (2003).
[20] F. Ghafoor, S. Y. Zhu, and M. S. Zubairy, Phys. Rev. A **62**, 013811 (2000).
[21] E. Paspalakis and P. L. Knight, Phys. Rev. Lett. **81**, 293 (1998); E. Paspalakis, N. J. Kylstra, and P. L. Knight, *ibid*. **82**, 2079 (1999); A. Fountoulakis, A. F. Terzis, and E. Paspalakis, Phys. Rev. A **73**, 033811 (2006).
[22] H. Lee, P. Polynkin, M. O. Scully, and S. Y. Zhu, Phys. Rev. A **55**, 4454 (1997).
[23] J. H. Wu, A. J. Li, Y. Ding, Y. C. Zhao, and J. Y. Gao, Phys. Rev. A **72**, 023802 (2005).
[24] W. Harshawardhan and G. S. Agarwal, Phys. Rev. A **53**, 1812 (1996).
[25] A. Joshi and M. Xiao, Phys. Rev. Lett. **91**, 143904 (2003).
[26] M. Holland, S. Marksteiner, P. Marte, and P. Zoller, Phys. Rev. Lett. **76**, 3683 (1996).
[27] F. LeKien, G. Rempe, W. P. Schleich, and M. S. Zubairy, Phys. Rev. A **56**, 2972 (1997).
[28] A. M. Herkommer, W. P. Schleich, and M. S. Zubairy, J. Mod. Opt. **44**, 2507 (1997).
[29] S. Qamar, S. Y. Zhu, and M. S. Zubairy, Phys. Rev. A **61**, 063806 (2000).
[30] E. Paspalakis and P. L. Knight, Phys. Rev. A **63**, 065802 (2001).
[31] E. Paspalakis, A. F. Terzis, and P. L. Knight, J. Mod. Opt. **52**, 1685 (2005).
[32] L. L. Jin, H. Sun, Y. P. Niu, and S. Q. Gong, J. Phys. B **41**, 085508 (2008).
[33] S. Qamar, A. Mehmood, and S. Qamar, Phys. Rev. A **79**, 033848 (2009).
[34] M. Sahrai, H. Tajalli, K. T. Kapale, and M. S. Zubairy, Phys. Rev. A **72**, 013820 (2005).
[35] K. T. Kapale and M. S. Zubairy, Phys. Rev. A **73**, 023813 (2006).
[36] D. C. Cheng, Y. P. Niu, R. X. Li, and S. Q. Gong, J. Opt. Soc. Am. B **23**, 2180 (2006).
[37] C. P. Liu, S. Q. Gong, D. C. Cheng, X. J. Fan, and Z. Z. Xu, Phys. Rev. A **73**, 025801 (2006).
[38] G. S. Agarwal and K. T. Kapale, J. Phys. B **39**, 3437 (2006).
[39] R. G. Wan, J. Kou, L. Jiang, Y. Jiang, and J. Y. Gao, J. Opt. Soc. Am. B **28**, 622 (2011).
[40] J. Evers, S. Qamar, and M. S. Zubairy, Phys. Rev. A **75**, 053809 (2007).
[41] L. L. Jin, H. Sun, Y. P. Niu, S. Q. Jin, and S. Q. Gong, J. Mod. Opt. **56**, 805 (2009).
[42] V. Ivanov and Y. Rozhdestvensky, Phys. Rev. A **81**, 033809 (2010).
[43] R. G. Wan, J. Kou, L. Jiang, Y. Jiang, and J. Y. Gao, Opt. Commun. **284**, 985 (2011).
[44] R. G. Wan, J. Kou, L. Jiang, Y. Jiang, and J. Y. Gao, J. Opt. Soc. Am. B **28**, 10 (2011).
[45] B. K. Dutta and P. K. Mahapatra, Opt. Commun. **282**, 594 (2009).
[46] P. Meystre and M. Sargent III, *Elements of Quantum Optics*, 3rd ed. (Springer-Verlag, Berlin, 1999).
[47] P. Lambropoulos, G. M. Nikolopoulos, T. R. Nielsen, and S. Bay, Rep. Prog. Phys. **63**, 455 (2000).